crystals

MDPI

Article

Room-Temperature Plastic Deformation of Strontium Titanate Crystals Grown from Different Chemical Compositions

Atsutomo Nakamura [1,*], Kensuke Yasufuku [1], Yuho Furushima [1], Kazuaki Toyoura [2], K. Peter D. Lagerlöf [3] and Katsuyuki Matsunaga [1,4]

1 Department of Materials Physics, Nagoya University, Furo-cho, Chikusa-ku, Nagoya 464-8603, Japan; keeenb9lox@gmail.com (K.Y.); furushima.yuuho@b.mbox.nagoya-u.ac.jp (Y.F.); kmatsunaga@nagoya-u.jp (K.M.)
2 Department of Materials Science and Engineering, Kyoto University, Yoshida Honmachi, Sakyo-ku, Kyoto 606-8501, Japan; toyoura.kazuaki.5r@kyoto-u.ac.jp
3 Department of Materials Science and Engineering, Case Western Reserve University, Cleveland, OH 44106, USA; peter.lagerlof@case.edu
4 Nanostructures Research Laboratory, Japan Fine Ceramics Center, 2-4-1, Mutsuno, Atsuta-ku, Nagoya 456-8587, Japan
* Correspondence: anaka@nagoya-u.jp; Tel.: +81-52-789-3366

Academic Editor: Helmut Cölfen
Received: 11 October 2017; Accepted: 21 November 2017; Published: 22 November 2017

Abstract: Oxide materials have the potential to exhibit superior mechanical properties in terms of high yield point, high melting point, and high chemical stability. Despite this, they are not widely used as a structural material due to their brittle nature. However, this study shows enhanced room-temperature plasticity of strontium titanate ($SrTiO_3$) crystals through the control of the chemical composition. It is shown that the deformation behavior of $SrTiO_3$ crystals at room temperature depends on the Sr/Ti ratio. It was found that flow stresses in deforming $SrTiO_3$ crystals grown from a powder with the particular ratio of $Sr/Ti = 1.04$ are almost independent of the strain rate because of the high mobility of dislocations in such crystals. As a result, the $SrTiO_3$ crystals can deform by dislocation slip up to a strain of more than 10%, even at a very high strain rate of 10% per second. It is thus demonstrated that $SrTiO_3$ crystals can exhibit excellent plasticity when chemical composition in the crystal is properly controlled.

Keywords: strontium titanate (STO); dislocations; transmission electron microscopy (TEM); single crystals; oxides

1. Introduction

Oxide crystals are typically brittle at low temperatures because of their predominant ionic and/or covalent bonding. It is known that slip systems that can be activated in ionic crystals are limited by electrostatic interactions between ions [1], whereas slip system activation in covalent crystals is affected by strongly localized and directional bonds that share electrons [2]. In addition, oxide crystals have large unit cells, leading to large lattice constants, since an oxide is a compound between one or more metallic elements and oxygen atoms. As a result, oxide crystals have large Burgers vectors, which represent the magnitude and direction of dislocations that produce plastic deformation. The larger Burgers vectors make it more difficult to move dislocations. Since the stresses required for dislocation motion are often larger than stresses required for crack propagation, oxide crystals are typically brittle by nature.

The mechanical properties of strontium titanate ($SrTiO_3$) crystals have received growing interest due to the fact that they can exhibit a large degree of plasticity even at low temperatures [3–11]. $SrTiO_3$ is an oxide with a cubic perovskite structure belonging to the $Pm\bar{3}m$ space group. It has been reported that $SrTiO_3$ crystals can plastically deform in temperature ranges from 78 K to 1050 K [3,4]. In addition, $SrTiO_3$ crystals can deform up to and over 10% if they deform at a slow strain rate of 10^{-4} (s^{-1}) [6,7]. Recently, the deformation behavior and dislocation structure have been reported to be temperature dependent [9]. In addition, Kondo et al. demonstrated using in-situ observation in transmission electron microscopy (TEM) that dislocation glide can take place in $SrTiO_3$ crystals even at room temperature [10,11]. Thus, $SrTiO_3$ crystals are believed to exhibit plasticity even at low temperatures due to mobility of dislocations belonging to the {110}<110> slip systems. However, there is still little known about any key factor providing the high dislocation mobility of $SrTiO_3$.

In the present study, $SrTiO_3$ single crystals grown from powders with varying Sr/Ti ratios were deformed at room temperature. This is believed to be due to the fact that a variety of point defects can be formed in $SrTiO_3$ crystals depending on the specific chemical composition and/or chemical environments around the crystals [12,13]. It is well known that point defects in a crystal can interact strongly with dislocations. In general, point defects act as barriers to dislocation motion and result in work hardening of materials followed by nucleation and growth of cracks, leading to brittle fracture. In fact, both Sr and O vacancies have been reported to be present around dislocations in $SrTiO_3$ [14–16], forming a Cottrell atmosphere [1]. However, the influence of point defects on the dislocation mobility in $SrTiO_3$ has not been examined.

2. Experimental

$SrTiO_3$ single crystals, grown by the Verneuil method from high purity $SrTiO_3$ powder (99.9 wt % and Sr/Ti = 1.002) and high purity $SrCO_3$ powder (99.99 wt %), were used for the present deformation experiments. Typically, Sr deficiency is induced during crystal growth of $SrTiO_3$ crystals due to the evaporation of Sr ahead of the solidification front [17]. In addition, Sr vacancies are easily formed in $SrTiO_3$ because of the low formation energy [12,13]. For this reason, single crystals grown with a non-stoichiometric starting powder having excess Sr ($Sr/Ti > 1$) would result in fewer Sr vacancies in the resultant $SrTiO_3$ crystal. Thus, single crystals grown using starting powders with two composition ratios, Sr/Ti = 1.00 and Sr/Ti = 1.04, respectively, were selected to be used in this study. As the starting powder of Sr/Ti = 1.00, 1000.00 g of the high purity $SrTiO_3$ powder was employed as it was. On the other hand, a mixed powder of 1000.00 g high purity $SrTiO_3$ powder and 32.18 g high purity $SrCO_3$ powder was employed as the starting powder of Sr/Ti = 1.04. The growing of all single crystals was performed using a Verneuil furnace at Shinkosha Co., Ltd. (Yokohama, Japan). Here, we note that, considering the evaporation loss of Sr, excess Sr does not necessarily exist even in the crystals grown from the powder with Sr/Ti = 1.04. Meanwhile, it is difficult to display the real atomic ratios of Sr/Ti in the grown crystals because a slight change in the ratios is buried in a mass of Sr and Ti atoms. The grown crystals from Sr/Ti = 1.04 should have fewer Sr vacancies than those from Sr/Ti = 1.00.

Figure 1 shows the shapes and crystallographic orientation of the specimens for deformation tests. Specimens were deformed by compression along [001] at strain rates of $\dot{\varepsilon} = 1.0 \times 10^{-5}$ (s^{-1}) and $\dot{\varepsilon} = 1.0 \times 10^{-1}$ (s^{-1}) in air at 297 K. Note that $\dot{\varepsilon} = 1.0 \times 10^{-1}$ (s^{-1}) is a high strain rate because specimens must change their length by 10% every second. In the case of the deformation along [001], four equivalent slip systems ((011)[0$\bar{1}$1], (0$\bar{1}$1)[011], (101)[$\bar{1}$01], and ($\bar{1}$01)[101], respectively, which are illustrated in Figure 1) are expected to be primary slip systems because they all have a Schmid factor equal to 0.5. During plastic deformation, the specimen's length and shape were recorded using a high-speed optical camera in order to confirm slip lines formed on their polished surfaces. The deformed crystals were examined by TEM (Hitachi H-800, 200 kV) to identify the density and type of dislocations that were introduced during the plastic deformation. Thin foils for TEM observations were prepared by a standard technique. That is, the specimens for deformation were mechanically sliced and ground to a thickness of about 60 μm and then attached with a stainless steel

single hole mesh for reinforcement. The center of the foils was milled by an Ar ion beam using an ion polishing system (Gatan PIPS II) to obtain electron transparency.

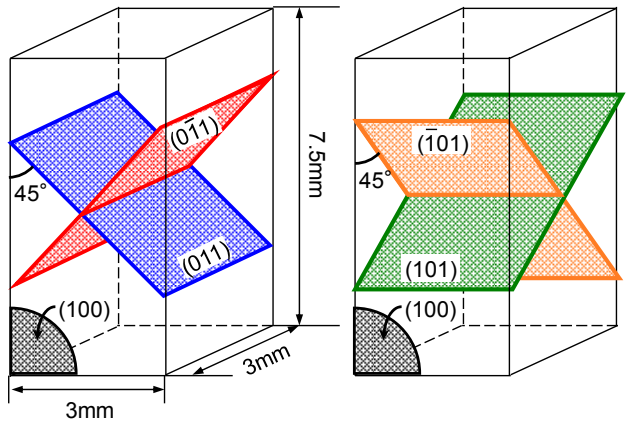

Figure 1. Schematic illustrations showing specimen shapes and available slip systems in the present deformation tests.

3. Results and Discussion

Figure 2a,b show the stress–strain curves that were obtained for the specimens with the two different chemical compositions of Sr/Ti = 1.00 (Figure 2a) and Sr/Ti = 1.04 (Figure 2b) as starting powders, respectively. It can be seen that stresses in all the curves gradually increase with increasing strain after yielding, and the deformed specimens give rise to brittle failure after a significant amount of work hardening. It was found that the Sr/Ti = 1.04 specimens exhibit lower yield and flow stresses as well as larger fracture strain, compared with the Sr/Ti = 1.00 specimens. The yield stresses, flow stresses (at a plastic strain of ε_p = 3%), and fracture strains of each specimen are shown in Table 1. As can be seen from the flow stresses at ε_p = 3%, the stress for Sr/Ti = 1.04 at $\dot{\varepsilon} = 1.0 \times 10^{-1}$ (s^{-1}) is higher by only 20% compared with the specimen deformed at $\dot{\varepsilon} = 1.0 \times 10^{-5}$ (s^{-1}), in spite of the fact that the strain rate is 10^4 times higher. In contrast, the stress for Sr/Ti = 1.00 increases by 31% with respect to the higher strain rate. The fracture stresses for the Sr/Ti = 1.04 specimens are significantly higher than those for the Sr/Ti = 1.00 specimens.

Table 1. Deformation stresses and fracture strains for $SrTiO_3$ single crystals.

Sr/Ti	Strain Rate (s^{-1})	Yield Stress (MPa)	Flow Stress (at ε_p = 3%) (MPa)	Fracture Strain (%)
1.04	1.0×10^{-5}	112	122	13.6
	1.0×10^{-1}	135	147	13.1
1.00	1.0×10^{-5}	119	138	7.4
	1.0×10^{-1}	160	180	8.5

Figure 3a,b show shapes and surface morphologies of the Sr/Ti = 1.00 and Sr/Ti = 1.04 specimens deformed at $\dot{\varepsilon} = 1.0 \times 10^{-1}$ (s^{-1}), respectively. In both specimen types, slip lines become evident at around ε_p = 3% and continue to be generated until failure. Thus, it is evident that slip lines are formed even at the high strain rate of $\dot{\varepsilon} = 1.0 \times 10^{-1}$ (s^{-1}), indicating prominent multiplication and glide motion of dislocations, although the Sr/Ti = 1.00 specimen fails at an earlier stage of deformation. These results are similar to those observed in ordinary single crystals deformed at a slower strain rate. It should be mentioned that the formed slip lines originate from two particular primary slip systems, namely, the two systems of (011)[0$\bar{1}$1] and (0$\bar{1}$1)[011] or the two systems of (101)[$\bar{1}$01] and ($\bar{1}$01)[101], although the Schmid factors for all four of the slip systems are equal. This means that either the two systems of (011)[0$\bar{1}$1] and (0$\bar{1}$1)[011] or the two systems of (101)[$\bar{1}$01] and ($\bar{1}$01)[101] are preferentially

activated during plastic deformation. As a result, only the horizontal slip lines were observed on a side surface of deformed specimens, as shown in Figure 3. This tendency is consistent with the previous reports [6,9] of plastic deformation of $SrTiO_3$ crystals.

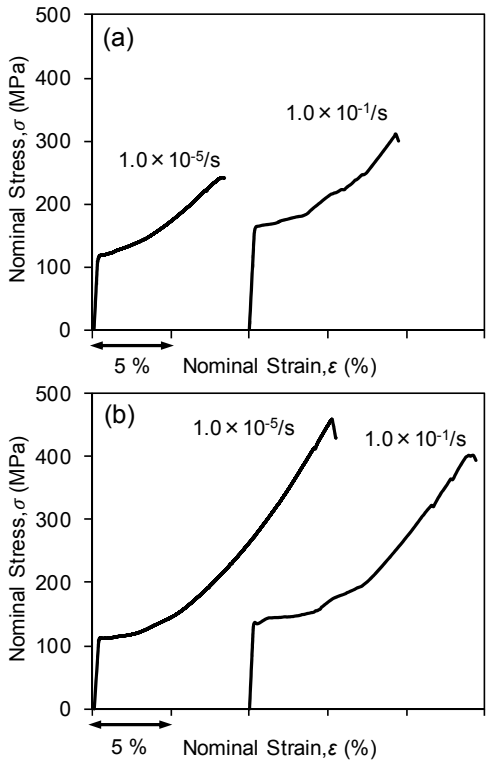

Figure 2. Stress–strain curves of $SrTiO_3$ single crystals with different chemical compositions, deformed at constant strain rates of $\dot{\varepsilon} = 1.0 \times 10^{-5}$ (s^{-1}) and $\dot{\varepsilon} = 1.0 \times 10^{-1}$ (s^{-1}). (**a**) $Sr/Ti = 1.00$, (**b**) $Sr/Ti = 1.04$ as the starting powders.

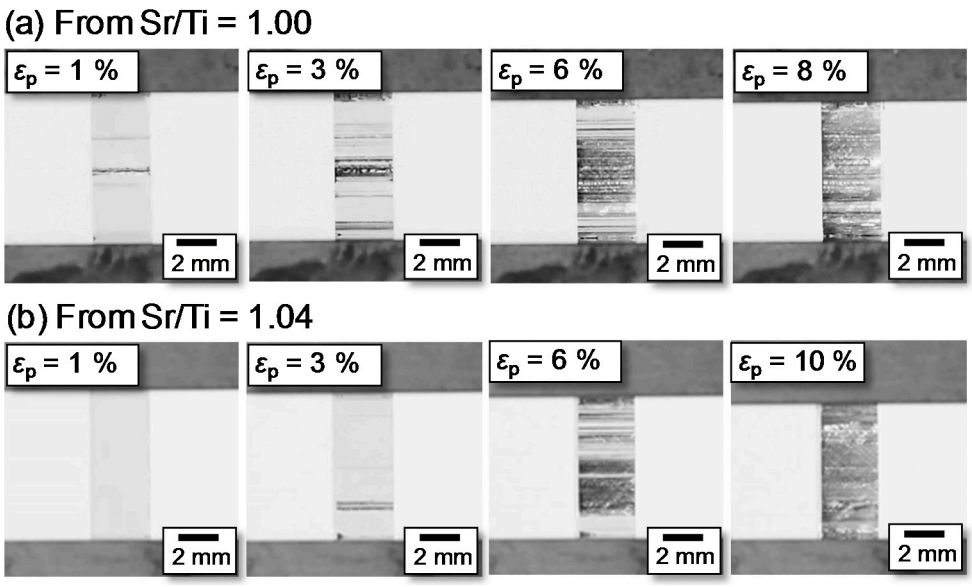

Figure 3. Shapes and surface morphologies of the deformed specimens. (**a**) The $Sr/Ti = 1.00$ specimen deformed at $\dot{\varepsilon} = 1.0 \times 10^{-1}$ (s^{-1}). (**b**) The $Sr/Ti = 1.04$ specimen deformed at $\dot{\varepsilon} = 1.0 \times 10^{-1}$ (s^{-1}). Here, each ε_p in the figures indicates the plastic strain.

Figure 4a,b show typical TEM bright field images taken from a Sr/Ti = 1.04 specimen deformed at $\dot{\varepsilon}$ = 1.0 × 10^{-1} (s^{-1}) up to ε_p = 3%. The incident beam direction is normal to the (011) primary slip plane, where the observed foil for TEM was prepared parallel to the slip lines formed by a primary slip system of (011)[0$\bar{1}$1]. It can be seen that many dislocations are introduced by the deformation, and most of the dislocations are present parallel to the (011) primary slip plane. Since glide dislocations in $SrTiO_3$ have Burgers vectors of the 1/2<011> type, the Burgers vectors of the dislocations in deformed specimens should be ±1/2[0$\bar{1}$1] according to activation of the (011)[0$\bar{1}$1] slip system. The image in Figure 4b is obtained from the same field as Figure 4a by using a different diffraction vector of $\boldsymbol{g}$ = 100. It can be seen that contrasts from almost all dislocations disappear under the diffraction vector of $\boldsymbol{g}$ = 100. This is because the ±1/2[0$\bar{1}$1] dislocations originating from the (011)[0$\bar{1}$1] slip system should lose contrasts according to the $\boldsymbol{g}\cdot\boldsymbol{b}$ = 0 condition [18]. Thus, the dislocation substructure formed by a deformation test is believed to be mainly formed due to the activation of a primary slip system.

Figure 5 represents the dislocation substructure of a Sr/Ti = 1.04 specimen deformed at $\dot{\varepsilon}$ = 1.0 × 10^{-5} (s^{-1}), which is also observed normally to the (011) primary slip plane. It can be also seen from the images that the density and type of introduced dislocations are almost same as those in the specimen deformed at $\dot{\varepsilon}$ = 1.0 × 10^{-1} (s^{-1}). It should be noticed from comparison of the dislocation substructures that the density and type of introduced dislocations are very similar in spite of the great difference in the given strain rates. Additionally, dislocation densities of the specimens deformed up to ε_p = 3% were about 1 × $10^{13}/m^2$, estimated using the Keh method [19] from the TEM images, regardless of given strain rates. The obtained dislocation densities are consistent with the values in earlier research [9], where the densities of dislocations in the un-deformed specimen and the specimen deformed up to 1% plastic strain at 25 °C were reported to be 3.7 × $10^{12}/m^2$ and 7.9 × $10^{12}/m^2$, respectively. In fact, since the difference in flow stresses is not great, as can be seen from the stresses at ε_p = 3% in Table 1, then it would be reasonable to conclude that dislocation densities were almost independent of given strain rates. Meanwhile, the image in Figure 6 shows the dislocation substructure of a Sr/Ti = 1.00 specimen deformed at $\dot{\varepsilon}$ = 1.0 × 10^{-5} (s^{-1}). The density and type of introduced dislocations are also similar, regardless of the difference in chemical compositions as starting powders. Consequently, it can be said that the ratio of Sr/Ti does not strongly affect the dislocation substructure.

From the above discussion, it has been shown that the yield and flow stresses become lower in the Sr/Ti = 1.04 specimens without changing the character of the dislocation substructures. The Sr/Ti = 1.00 specimens are believed to have more point defects, such as Sr vacancies and Ti anti-sites that substitute for Sr, since Sr deficiency should be induced through Sr evaporation during crystal growth. Conversely, it is plausible that the Sr/Ti = 1.04 specimens have a composition that is closer to the stoichiometric composition in a grown crystal. A more stoichiometric composition in the grown crystal will give rise to fewer point defects, resulting in less interaction with moving dislocations. This may be the reason why the Sr/Ti = 1.04 specimens exhibit lower yield and flow stresses.

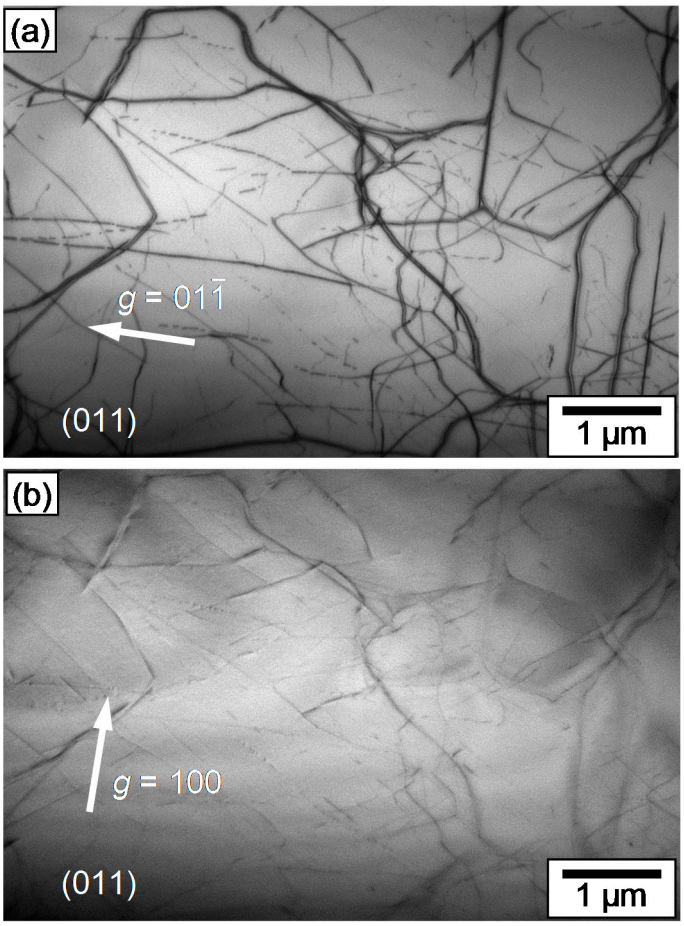

Figure 4. Typical TEM bright field images taken from the Sr/Ti = 1.04 specimen deformed at $\dot{\varepsilon}$ = 1.0 × 10^{-1} (s^{-1}) up to ε_p = 3%. The image in (**b**) was obtained from the same field as in (**a**) using a different diffraction vector.

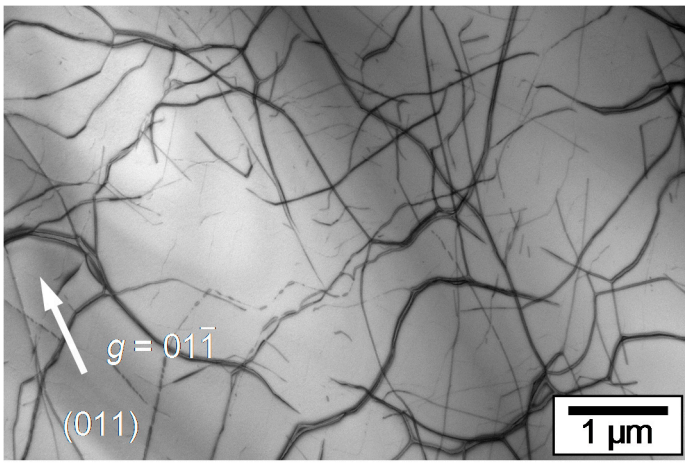

Figure 5. A typical TEM bright field image taken from the Sr/Ti = 1.04 specimen deformed at $\dot{\varepsilon}$ = 1.0 × 10^{-5} (s^{-1}) up to ε_p = 3%.

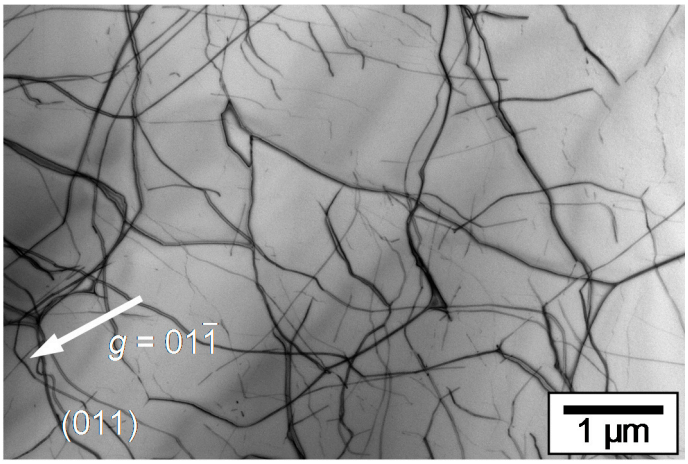

Figure 6. A typical TEM bright field image taken from the Sr/Ti = 1.00 specimen deformed at $\dot{\varepsilon} = 1.0 \times 10^{-5}$ (s^{-1}) up to ε_p = 3%.

It is interesting to note that strain-rate dependency of the deformation stress is small for both the Sr/Ti = 1.00 and Sr/Ti = 1.04 specimens, although the degree is more prominent in the case of Sr/Ti = 1.04. In order to evaluate the strain-rate dependency with respect to dislocation velocity in these specimens, an analysis will be done based on the Orowan relationship [1],

$$\dot{\gamma} = \rho b \overline{v} \tag{1}$$

where $\dot{\gamma}$ is the shear strain rate, ρ is the density of mobile dislocations, b is the magnitude of the Burgers vector of the mobile dislocations, and $\overline{v}$ is the average motion speed of the mobile dislocations. In addition, the relation between $\overline{v}$ and deformation stress is given by

$$\overline{v} \approx \tau^m \tag{2}$$

where τ is the shear stress and m is the stress exponent [20,21]. As can be seen from TEM images at ε_p = 3% in Figures 4 and 5, the dislocation densities of deformed specimens are similar even after increasing the strain rate by a factor of 10^4. Here, we note that dislocations that are observable in the TEM include both mobile and immobile dislocations, and most of the observable dislocations in some cases can be immobile [22]. Accordingly, the densities of mobile dislocations in deforming specimens are still unknown. First of all, we assume that the density of mobile dislocations should be independent of the strain rate as the dislocation substructures introduced by the deformation tests are very similar in spite of great difference in the given strain rates. In this assumption, the dislocation velocity of the mobile dislocations—$\overline{v}$ in Equation (1)—must increase by a factor of 10^4 in the case of the high strain rate of $\dot{\varepsilon} = 1.0 \times 10^{-1}$ (s^{-1}) since the strain rate, $\dot{\gamma}$, should be proportional to the dislocation velocity, $\overline{v}$. Moreover, since the flow stresses at ε_p = 3% have been determined (see Figure 1 and Table 1) for both cases of $\dot{\varepsilon} = 1.0 \times 10^{-5}$ (s^{-1}) and $\dot{\varepsilon} = 1.0 \times 10^{-1}$ (s^{-1}), the stress exponent m for $SrTiO_3$ crystals with a particular chemical composition can be estimated by using Equation (2). The values of m in this assumption are calculated to be 35 and 49 for the Sr/Ti = 1.00 and Sr/Ti = 1.04 specimens, respectively. Next, we assume that the density of mobile dislocations depends on the strain rate. Two hypotheses were considered: (i) there are ten times as many mobile dislocations, and (ii) there are one-tenth as many mobile dislocations in the case of the high strain rate of 1.0×10^{-1} (s^{-1}). Even in these hypothetical situations, the value of m can be estimated by using Equations (1) and (2). The values of m derived from (i) i.e., the hypothesis of ten times as many mobile dislocations, can be calculated to be 26 and 37 for the Sr/Ti = 1.00 and Sr/Ti = 1.04 specimens, respectively. Meanwhile, the values of m derived from (ii) i.e., the hypothesis of one-tenth as many mobile dislocations can be

calculated to be 43 and 62 for the Sr/Ti = 1.00 and Sr/Ti = 1.04 specimens, respectively. Although the m in Equation (2) mainly depends on deformation flow stresses, the obtained values of m still have a dependency on the densities of mobile dislocations for each of the strain rates. Nevertheless, it is worth pointing out the fact that the stress exponent m for most crystalline materials, including metals, is less than 10 [21]. The m for $SrTiO_3$ would have definitely high values although there is still room for argument about the densities of mobile dislocations. Regardless, it can be said that the dislocation dynamics in $SrTiO_3$ single crystals are remarkable and interesting. We note that a higher value of stress exponent corresponds to smaller strain-rate dependency of deformation flow stresses. In addition, it can be seen from Equation (2) that a larger value of the stress exponent, m, results in a higher value of the dislocation velocity of the mobile dislocations, $\overline{v}$, for the same stress level, τ. That is, the dislocations in the Sr/Ti = 1.04 specimens would have higher mobility as compared with the dislocations in the Sr/Ti = 1.00 specimens. This is believed to be due to fewer point defects for a $SrTiO_3$ crystal made from a starting powder with Sr/Ti = 1.04.

Finally, the larger fracture stresses for crystals made from a starting powder with Sr/Ti = 1.04 will be considered. As seen from Figure 2, fracture stresses for the Sr/Ti = 1.04 specimens are significantly larger than those for the Sr/Ti = 1.00 specimens. As mentioned previously, the mobility of dislocations for the Sr/Ti = 1.04 specimens is significantly higher than that for the Sr/Ti = 1.00 specimens. The higher dislocation mobility can reduce stress concentrations during plastic deforming since the dislocations can accommodate the applied stress. The larger fracture stresses for the Sr/Ti = 1.04 specimens would arise from the higher dislocation mobility. In contrast, the Sr/Ti = 1.00 specimens fail at lower stresses. This can be explained by the relatively lower dislocation mobility, which has a potential to induce higher stress concentrations during plastic deformation.

4. Conclusions

From deformation tests of $SrTiO_3$ single crystals, it was found that a crystal grown with the ratio of Sr/Ti = 1.04 as the starting powder can deform with a high degree of plasticity up to a strain of more than 10% at room temperature, even at a very high strain rate of $\dot{\varepsilon}$ = 0.1 (s^{-1}). It is remarkable that the strain-rate dependency of deformation flow stress in $SrTiO_3$ is rather small, in particular for crystals made from powders with Sr/Ti = 1.04, meaning that dislocations exhibit a relatively high mobility in these crystals. As a result, larger fracture stresses and strains could be attained for the Sr/Ti = 1.04 specimens. Here, it should be also mentioned that it is still unclear whether the crystals grown with the ratio of Sr/Ti = 1.04 exhibit the highest plasticity or not. Namely, there is a possibility that a better composition of powders for higher plasticity of $SrTiO_3$ crystals will be found in the future. It is likely that the crystals grown from Sr/Ti = 1.04 should have fewer Sr vacancies than those from Sr/Ti = 1.00, since additional Sr elements are mixed with the starting powder. Moreover, the crystals from Sr/Ti = 1.04 exhibited higher plasticity as an actual fact. It can be said that the plasticity of $SrTiO_3$ crystals could be enhanced if the chemical composition is properly controlled so as to decrease point defects in a crystal. This suggests that it may be possible to enhance the plasticity of other oxide materials by controlling the chemical composition and resulting point defect populations.

Acknowledgments: The authors gratefully acknowledge the financial support by a Grant-in-Aid for Scientific Research on Innovative Areas "Nano Informatics" (JP25106002) from Japan Society for the Promotion of Science (JSPS). A part of this study was supported by JSPS KAKENHI Grant Numbers JP15H04145, JP16K14414, JP17H06094 and JP17K18983. A.N. also thanks Iketani Science and Technology Foundation for the financial support. Additionally, this work was partly supported by Nanotechnology Platform Program (Advanced Characterization Nanotechnology Platforms of Nagoya Univ.) of the Ministry of Education, Culture, Sports, Science and Technology (MEXT), Japan.

Author Contributions: Atsutomo Nakamura and Katsuyuki Matsunaga conceived the research idea, and Atsutomo Nakamura designed the experiments; Kensuke Yasufuku, Yuho Furushima, and Atsutomo Nakamura performed the experiments and analyzed the data; K. Peter D. Lagerlöf, Kazuaki Toyoura, and Katsuyuki Matsunaga advised the experiments; all authors discussed the results and wrote the paper.

Conflicts of Interest: The authors declare no competing financial interests.

References

1. Hirth, J.P.; Lothe, L. *Theory of Dislocations*, 2nd ed.; Wiley: New York, NY, USA, 1982.
2. Hull, D.; Bacon, D.J. *Introduction to Dislocations*; Elsevier: Oxford, UK, 2011; pp. 124–133.
3. Brunner, D.; Taeri-Baghbadrani, S.; Sigle, W.; Ruhle, M. Surprising Results of a Study on the Plasticity in Strontium Titanate. *J. Am. Ceram. Soc.* **2001**, *84*, 1161–1163. [CrossRef]
4. Gumbsch, P.; Taeri-Baghbadrani, S.; Brunner, D.; Sigle, W.; Ruhle, M. Plasticity and an inverse brittle-to-ductile transition in strontium titanate. *Phys. Rev. Lett.* **2001**, *87*, 085505. [CrossRef] [PubMed]
5. Taeri, S.; Brunner, D.; Sigle, W.; Rühle, M. Deformation behaviour of strontium titanate between room temperature and 1800 K under ambient pressure. *Z. Metall.* **2004**, *95*, 433–446. [CrossRef]
6. Brunner, D. Low-temperature plasticity and flow-stress behaviour of strontium titanate single crystals. *Acta Mater.* **2006**, *54*, 4999–5011. [CrossRef]
7. Sigle, W.; Sarbu, C.; Brunner, D.; Ruhle, M. Dislocations in plastically deformed $SrTiO_3$. *Philos. Mag.* **2006**, *86*, 4809–4821. [CrossRef]
8. Yang, K.-H.; Ho, N.-J.; Lu, H.-Y. Plastic Deformation of <001> Single-Crystal $SrTiO_3$ by Compression at Room Temperature. *J. Am. Ceram. Soc.* **2011**, *94*, 3104–3111. [CrossRef]
9. Patterson, E.A.; Major, M.; Donner, W.; Durst, K.; Webber, K.G.; Rodel, J. Temperature-Dependent deformation and dislocation density in $SrTiO_3$ (001) single crystals. *J. Am. Ceram. Soc.* **2016**, *99*, 3411–3420. [CrossRef]
10. Kondo, S.; Shibata, N.; Mitsuma, T.; Tochigi, E.; Ikuhara, Y. Dynamic observations of dislocation behavior in $SrTiO_3$ by in situ nanoindentation in a transmission electron microscope. *Appl. Phys. Lett.* **2012**, *100*, 181906. [CrossRef]
11. Kondo, S.; Mitsuma, T.; Shibata, N.; Ikuhara, Y. Direct observation of individual dislocation interaction processes with grain boundaries. *Sci. Adv.* **2016**, *2*, e1501926. [CrossRef] [PubMed]
12. Tanaka, T.; Matsunaga, K.; Ikuhara, Y.; Yamamoto, T. First-principles study on structures and energetics of intrinsic vacancies in $SrTiO_3$. *Phys. Rev. B* **2003**, *68*, 205213. [CrossRef]
13. Liu, B.; Cooper, V.; Xu, H.; Xiao, H.; Zhang, Y.; Weber, W. Composition dependent intrinsic defect structures in $SrTiO_3$. *Phys. Chem. Chem. Phys.* **2014**, *16*, 15590–15596. [CrossRef] [PubMed]
14. Takehara, K.; Sato, Y.; Tohei, T.; Shibata, N.; Ikuhara, Y. Titanium enrichment and strontium depletion near edge dislocation in strontium titanate [001]/(110) low-angle tilt grain boundary. *J. Mater. Sci.* **2014**, *49*, 3962–3969. [CrossRef]
15. Choi, S.Y.; Kim, S.D.; Choi, M.; Lee, H.S.; Ryu, J.; Shibata, N.; Mizoguchi, T.; Tochigi, E.; Yamamoto, T.; Kang, S.J.L. Assessment of strain-generated oxygen vacancies using $SrTiO_3$ bicrystals. *Nano Lett.* **2015**, *15*, 4129–4134. [CrossRef] [PubMed]
16. Furushima, Y.; Arakawa, Y.; Nakamura, A.; Tochigi, E.; Matsunaga, K. Nonstoichiometric [012] dislocation in strontium titanate. *Acta Mater.* **2017**, *135*, 103–111. [CrossRef]
17. Scheel, H.J.; Bednorz, J.G.; Dill, P. Crystal growth of strontium titanate. *Ferroelectrics* **1976**, *13*, 507–509. [CrossRef]
18. Williams, D.B.; Carter, C.B. *Transmission Electron Microscopy: A Textbook for Materials Science*, 2nd ed.; Springer: New York, NY, USA, 2009.
19. Keh, A.S. Dislocation Arrangement in Alpha Iron during Deformation and Recovery. In *Direct Observation of Imperfections in Crystal*; Interscience Publishers (Wiley): New York, NY, USA, 1961.
20. Messerschmidt, U. *Dislocation Dynamics during Plastic Deformation*; Springer: Berlin, Germany, 2010; pp. 73–280.
21. Nadgornyi, E. *Dislocation Dynamics and Mechanical Properties of Crystals*; Pergamon: Oxford, UK, 1988; pp. 1–536.
22. Bergsröm, Y. A dislocation model for the stress-strain behaviour of polycrystalline α-Fe with special emphasis on the variation of the densities of mobile and immobile dislocations. *Mater. Sci. Eng.* **1970**, *5*, 193–200. [CrossRef]

© 2017 by the authors. Licensee MDPI, Basel, Switzerland. This article is an open access article distributed under the terms and conditions of the Creative Commons Attribution (CC BY) license (http://creativecommons.org/licenses/by/4.0/).